Determination of magnetic-moment directions using x-ray resonant exchange scattering

C. Detlefs, A. H. M. Z. Islam, A. I. Goldman, C. Stassis, and P. C. Canfield
Ames Laboratory and Department of Physics and Astronomy, Iowa State University, Ames, Iowa 50011

J. P. Hill and D. Gibbs
Department of Physics, Brookhaven National Laboratory, Upton, New York 11973
(Received 7 October 1996)

We present determinations of the magnetic structures of $NdNi_2B_2C$ and $SmNi_2B_2C$ by means of x-ray resonant exchange scattering (XRES). The integrated intensity of a number of magnetic reflections was measured as a function of the Bragg angle and compared to model calculations for various magnetic structures. The two compounds were found to have the same magnetic modulation wave vector but different moment directions. A resonant feature observed below the Sm L_3-absorption edge, similar to unexplained effects found in other light rare-earth compounds, is identified as quadrupolar XRES and is used to refine the details of the moment direction. [S0163-1829(97)50602-3]

The discovery of large resonant enhancements in the x-ray magnetic scattering cross section when the incident photon energy is tuned to an atomic absorption edge[1,2] has greatly increased the potential of x-ray magnetic scattering in materials characterization. The majority of experiments performed so far have utilized the enhancements to determine the temperature dependence of order parameters or to perform high-resolution measurements of the magnetic modulation wave vector. Recently, detailed evaluations of the x-ray resonant exchange scattering (XRES) cross section[3–5] have triggered attempts to exploit the polarization dependence of the cross section to extract magnetic structure information.[6,7]

The ability of resonant x-ray scattering to determine moment directions would be of great utility for materials which are not amenable to conventional neutron scattering techniques, for example those that contain neutron opaque elements (Sm, Gd, etc.) or very small samples. The element specificity of the technique makes it particularly interesting for mixed spin systems, since, in principle, it is possible to determine the temperature dependence and direction of the ordered moment of each sublattice with a model-independent procedure, in contrast to neutron-scattering methods. In addition, x-ray resonant scattering offers the ability to study surface magnetism,[8] and the potential to resolve orbital and spin contributions through the use of sum rules.[4]

In this paper, we demonstrate that it is possible to determine moment directions using resonant x-ray magnetic scattering. We have chosen to study two related compounds, $NdNi_2B_2C$ and $SmNi_2B_2C$, both of which order in a commensurate antiferromagnetic structure with propagation vector $(\frac{1}{2},0,\frac{1}{2})$. These materials are interesting as members of the recently discovered[9,10] rare-earth nickel boron carbide family, which includes some antiferromagnetic superconductors.

The structure of the rare-earth nickel boron carbides is tetragonal (space group $I4/mmm$), consisting of RC layers separated by Ni_2B_2 sheets, where R=rare-earth.[10] At low temperatures, superconductivity coexists with long-range antiferromagnetic order for some of the heavy R ions, including Tm, Er, Ho, and Dy. No superconductivity has been observed for the light R members, down to 2 K. Nevertheless, their magnetic properties are of great interest and several neutron and x-ray scattering experiments[11] have revealed a broad range of magnetic structures.

Single crystals of $NdNi_2B_2C$ and $SmNi_2B_2C$ were grown at Ames Laboratory using a high-temperature-flux-growth technique.[12] The face perpendicular to the c axis of each sample was mechanically polished. The crystals were then annealed at 900 °C in a vacuum of 10^{-7} Torr for 36 h. The sample dimensions were approximately $3\times0.7\times0.1$ mm^3 for the Nd compound and $2\times1.3\times0.1$ mm^3 for the Sm compound.

The experiments were carried out at beamline X22C of the National Synchrotron Light Source, using a Ge(111) double crystal monochromator and a Ge(111) analyzer. A Ni-coated toroidal focusing mirror eliminated higher harmonics in the incident beam. The samples were mounted in a closed cycle refrigerator such that the $(h0l)$ zone was coincident with the diffraction plane (Fig. 1). The mosaic spreads of the $(00l)$ reflections were approximately 0.09° and 0.14° full width at half maximum for the Nd and Sm compounds, respectively.

For the sample orientation shown in Fig. 1, the x-ray resonant scattering cross section (the nonresonant scattering contribution was observed to be negligible) may be written as

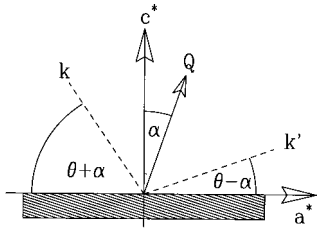

FIG. 1. The scattering geometry used in the present measurements with respect to the a, b, and c axes of the sample. The incident x-ray polarization is directed out of the scattering plane (σ polarization), along the b axis. The alignment of the crystal was such that reflections $(h,0,l)$ with positive index $h>0$ have positive asymmetry angles, $\alpha>0$.

$$I \propto \left| \sum_n e^{i\mathbf{Q}\cdot\mathbf{r}_n} F_n^{\mathrm{XRES}}(\mathbf{k},\hat{\epsilon},\mathbf{k}',\hat{\epsilon}',\hat{z}_n) \right|^2 \times \frac{\sin(\theta+\alpha)\sin(\theta-\alpha)}{2\mu\sin(\theta)\cos(\alpha)\sin(2\theta)}. \quad (1)$$

Here $\mathbf{k},\hat{\epsilon}$ and $\mathbf{k}',\hat{\epsilon}'$ are the wave vector and polarization of the incident and scattered x-ray beams, respectively, and $\hat{z}_n$ is the moment direction at nth site. α represents the ''asymmetry'' angle between the scattering vector, $\mathbf{Q}=\mathbf{k}'-\mathbf{k}$, and the surface normal, $\mathbf{c}^\star$ (Fig. 1). μ is the linear absorption coefficient and 2θ is the scattering angle. The Lorentz factor, $1/\sin(2\theta)$, as well as an angular factor required to correct for the fraction of the incident beam intercepted by the sample, $\sin(\theta+\alpha)$, are included to allow a comparison between the calculated cross section and the measured integrated intensity, I. The resonant scattering amplitude, F_n^{XRES} contains both dipole ($E1$) and quadrupole ($E2$) resonances, with the former typically dominant. At the R $L_{2,3}$-edges, these correspond to $2p\leftrightarrow 5d$ and $2p\leftrightarrow 4f$ transitions, respectively. The $E2$ transition is generally observed a few eV below the absorption edge, due to the stronger core-hole – excited electron interaction in the intermediate state. The two processes contribute distinct angular factors and it is these which we will exploit to determine the moment directions.

The $E1$ resonances produce first- and second-order harmonic satellites of the charge peaks, while $E2$ resonances give rise to satellites of up to fourth-order.[2,3] For a commensurate antiferromagnet the odd orders contribute to the magnetic scattering and we need only consider terms of first and third-order in $\hat{z}_n$. For the present experiment, with a σ-polarized incident beam (i.e., perpendicular to the scattering plane), these are[5]

$$F_{E1,\,1\mathrm{st}}^{\mathrm{XRES}}(\mathbf{k},\mathbf{k}') = -iF_{E1}^{(1)}\begin{pmatrix} 0 \\ -D' \end{pmatrix}, \quad (2)$$

$$F_{E2,\,1\mathrm{st}}^{\mathrm{XRES}}(\mathbf{k},\mathbf{k}') = -iF_{E2}^{(1)}\begin{pmatrix} C \\ -\cos(2\theta)D' \end{pmatrix}, \quad (3)$$

$$F_{E2,\,3\mathrm{rd}}^{\mathrm{XRES}}(\mathbf{k},\mathbf{k}') = -i\frac{F_{E2}^{(3)}-F_{E2}^{(1)}}{\sin^2(2\theta)}\begin{pmatrix} C^3 \\ -D'D\sin^2(2\theta)-C^2[D-\cos(2\theta)D'] \end{pmatrix} - i\frac{F_{E2}^{(3)}}{\sin^2(2\theta)}\begin{pmatrix} C[2\cos(2\theta)D'D-(D')^2-D^2] \\ C^2\cos(2\theta)D'+D[D-\cos(2\theta)D']^2 \end{pmatrix}, \quad (4)$$

where we have adopted a column vector notation, such that the top element describes the $\sigma\rightarrow\sigma$ scattering and the bottom element the $\sigma\rightarrow\pi$ scattering. $C:=(\hat{k}'\times\hat{k})\cdot\hat{z}_n$, $D:=\hat{k}\cdot\hat{z}_n$, and $D':=\hat{k}'\cdot\hat{z}_n$. The amplitude factors, $F_{E1}^{(1)}$ $F_{E2}^{(1)}$ and $F_{E2}^{(3)}$ are a combination of Clebsch-Gordan coefficients, the resonant energy denominator and radial dipole or quadrupole matrix elements, respectively.[5] They are independent of the scattering geometry.

A few points regarding the present scattering geometry are in order. First, in the absence of an in-plane (π) polarized component of the incident beam, the $E1$ terms are not sensitive to the component of the ordered moment perpendicular to the scattering plane (i.e., along the b axis). Second, the magnetic scattering intensity is not symmetric in α, in contrast to charge scattering for which the intensities are identical for reflections at α and $-\alpha$ [$(\pm h0l)$ Bragg peaks].

We first investigated $NdNi_2B_2C$, for which the modulation wave vector is known to be $(\frac{1}{2},0,\frac{1}{2})$ with the moment direction along the (100) direction.[13] The measurements were made at the maximum of the Nd L_2 resonance. Above the Néel temperature, $T_N=4.5$ K,[14] only charge reflections (h,k,l) with $h+k+l=2n$ were observed. The resonant scattering at the Nd L_3 energy was too weak to be observed in these measurements. Below T_N, satellites of the charge peaks appeared at $(h,k,l)\pm\mathbf{q}$ with $\mathbf{q}=(\frac{1}{2},0,\frac{1}{2})$. Peak intensities were $\sim$50 counts s^{-1}. The integrated intensities of pairs of equivalent satellites, $(\pm\frac{1}{2},0,l)$, corresponding to opposite asymmetry angles, $\pm\alpha$, were measured at $T=3.7$ K by performing rocking scans with the analyzer crystal removed and the detector slits set to accept the full scattered beam. These data were then numerically integrated.[7] The results of such a procedure are plotted as open circles in Fig. 2, together with the calculated dipole integrated intensity (dashed line) from Eqs. (1) and (2) for $\hat{z}_n\|(1,0,0)$. The data are well described by such a structure and we conclude that our results are consistent with the neutron work,[13] with the caveat that, for dipolar transitions, the x-ray measurement is not sensitive to any b-axis component of the magnetic moment.

With this reassurance, we next turn to $SmNi_2B_2C$, for which there is no previous microscopic information. In scans taken along the high-symmetry directions below the Néel temperature, $T_N=9.8$ K,[14] magnetic satellites were again observed at $(h,k,l)\pm\mathbf{q}$, with $\mathbf{q}=(\frac{1}{2},0,\frac{1}{2})$. The integrated intensities of the magnetic reflections were recorded at the L_2 resonance and are plotted in Fig. 2 (closed circles), along with the calculated dipole scattering from a moment parallel to (0,0,1) (solid line). While both compounds have the same modulation wave vector, their integrated intensities exhibit strikingly different behaviors as a function of the scattering angle. These differences result entirely from the different moment orientations in the two compounds and demonstrate the sensitivity of this technique to the moment direction.

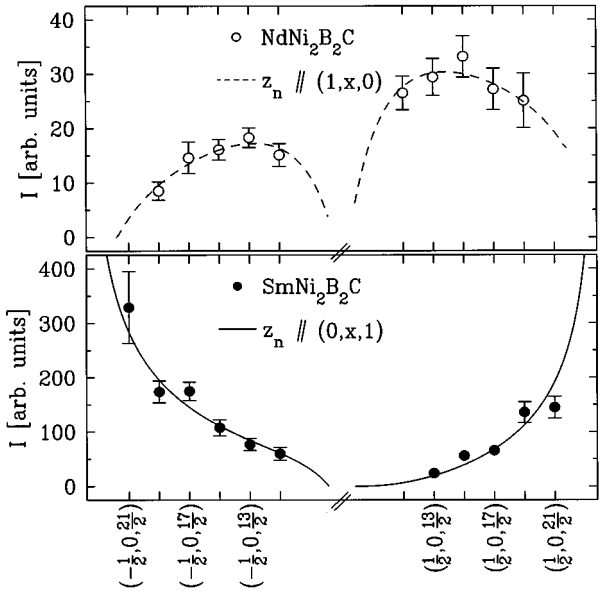

FIG. 2. The integrated intensity of magnetic reflections of $SmNi_2B_2C$ (●) and $NdNi_2B_2C$ (○) along with model calculations for a magnetic moment parallel to the *c* (—) and *a* (---) axes of the samples. The symbol *x* is used to remind the reader that these measurements are not sensitive to components of the magnetic moment along the *b*-axes.

Both sets of data are well described by Eqs. (1) and (2), assuming a magnetic moment direction along $(1,x,0)$ for $NdNi_2B_2C$ and along $(0,x,1)$ for $SmNi_2B_2C$, with only one adjustable parameter (the overall amplitude) for each sample. Due to the multipole expansion in the single-atom matrix elements, the XRES scattering amplitude is a discrete sum rather than a continuous Fourier transform of the moment density, so that no magnetic form factor is required to fit the data.[3]

A second, independent data set was then obtained for $SmNi_2B_2C$ at the Sm L_3-absorption edge. As for pure Sm,[15] the resonant signal at the Sm L_3 edge was roughly one order of magnitude weaker than at the L_2 edge. Further, as observed in other light rare-earth compounds,[15,16] energy scans across the Sm L_3-edge showed two separate peaks. These scans are shown in Fig. 3, uncorrected for absorption effects. The double peak structure is present at all satellites, $(-\frac{1}{2},0,l)$, though the relative intensity of the low-energy peak decreases with increasing Bragg angle.

The angular dependence of this lower energy resonance is a clear indication that it does *not* originate from $E1$ transitions (compare with Fig. 2) and we therefore ascribe it to $E2$ processes.[2] The intensity ratio of the two L_3 features was extracted for each magnetic Bragg reflection by fitting the data to a sum of two Lorentzian-squared functions and is plotted in Fig. 4. We may compare this to the theoretical quadrupole to dipole ratio, which is proportional to $|(F^{\mathrm{XRES}}_{E2,\,1\mathrm{st.}}+F^{\mathrm{XRES}}_{E2,3\mathrm{rd}})/F^{\mathrm{XRES}}_{E1,1\mathrm{st.}}|^2$, remembering that for $\mathbf{q}=(\frac{1}{2},0,\frac{1}{2})$ the first and the third harmonic satellites coincide.

The $E2$ amplitude factors, $F^{(1)}_{E2}$ and $F^{(3)}_{E2}$ may be approximated by their free-ion values, since they describe intra-atomic transitions $(2p\leftrightarrow 4f)$. We have used $F^{(1)}_{E2}/F^{(3)}_{E2}=2$.[17,18] The only adjustable parameter is then an

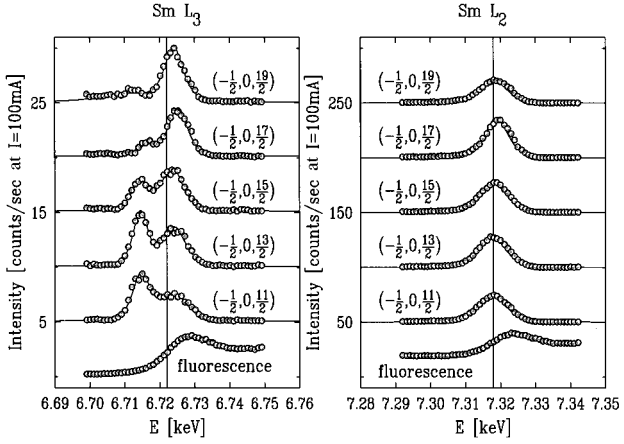

FIG. 3. Energy scans of the $(-\frac{1}{2},0,l)$ magnetic reflection across the Sm $L_{2,3}$ absorption edges. The fluorescence yield is plotted as an energy reference. Note that an absorption correction (not performed) would strongly increase the $E1$ features above the edge. The solid lines represent fits to the Sm L_3 (Sm L_2) data using two (one) Lorentzian-squared line shapes, respectively.

overall amplitude proportional to $F^{(1)}_{E2}/F^{(1)}_{E1}$. Note that an absorption correction, which has not been performed, would affect only this factor. The solid line in Fig. 4 is the result of such a calculation for an ordered moment along the (0,0,1) direction. The dot-dashed line represents the result of the same calculation for a moment along the (0,1,1) direction. Clearly the latter does not fit the data satisfactorily. A least-squares fit to the data reveals that the magnetic moments lie within about 20° of the *c* axis. Thus, by measuring the quadrupolar scattering, which is sensitive to a *b*-axis spin component, we can conclude that – within the accuracy of our measurement – the moments are along the (0,0,1) direction in $SmNi_2B_2C$.

We note that there are no indications of quadrupolar contributions to the Sm L_2 resonance. This is consistent with calculations which indicate that the absolute quadrupolar contributions to the L_2 resonant signal is ~4 times weaker than at the L_3 edge.[18]

In summary, x-ray resonant exchange scattering was observed at the Nd L_2-absorption edge in $NdNi_2B_2C$ and both

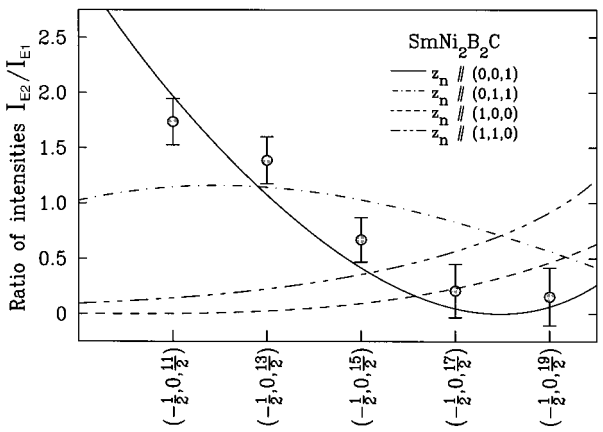

FIG. 4. The ratio of the intensities of dipolar and quadrupolar scattering along with model calculations for several directions of the magnetic moments.

the Sm L_2- and L_3-absorption edges in $SmNi_2B_2C$. Below their respective Néel temperatures, $T_N = 4.5$ and 9.8 K, the compounds order antiferromagnetically with a modulation wave vector of $\mathbf{q}=(\frac{1}{2},0,\frac{1}{2})$ [or the tetragonally equivalent $\mathbf{q}=(0,\frac{1}{2},\frac{1}{2})$]. The angular dependence of the resonant scattering intensity was used to determine the direction of the magnetic moments. A second resonant peak observed below the Sm L_3-absorption edge in energy scans of the magnetic reflections was attributed to quadrupolar transitions. This leads us to believe that similar L_3 features observed in pure Sm (Ref. 15) and several Nd compounds[16] are also quadrupolar in origin.

Finally, the significance of this work lies in the demonstration of the ability of x-ray resonant exchange scattering to determine moment directions with no *a priori* information. It is hoped that these results will extend the utility of the technique in future works.

The authors are grateful to B. N. Harmon and P. Carra for many stimulating discussions. We would also like to thank H. König for his calculation of the atomic $E2$ matrix elements for Sm^{3+}. Ames Laboratory is operated by the U.S. Department of Energy at Iowa State University under Contract No. W-7405-Eng-82. This work was supported by the Director for Energy Research, Office of Basic Sciences. The work at Brookhaven National Laboratory was carried out under Contract No. DE-AC02-76CH00016, Division of Materials Science, U.S. Department of Energy.

[1] D. H. Templeton and L. K. Templeton, Acta Crystallogr. Sec. A **36**, 237 (1980); K. Namikawa, M. Ando, T. Nakajima, and H. Kawata, J. Phys. Soc. Jpn. **54**, 4099 (1985); D. Gibbs, D. R. Harshmann, E. D. Isaacs, D. B. McWhan, D. Mills, and C. Vettier, Phys. Rev. Lett. **61**, 1241 (1988); E. D. Isaacs *et al.*, *ibid.* **62**, 1671 (1989).

[2] D. Gibbs *et al.*, Phys. Rev. B **43**, 5663 (1991).

[3] J. P. Hannon, G. T. Trammel, M. Blume, and D. Gibbs, Phys. Rev. Lett. **61**, 1245 (1988).

[4] P. Carra and B. T. Thole, Rev. Mod. Phys. **66**, 1509 (1994); Jin Luo, G. T. Trammel, and J. P. Hannon, Phys. Rev. Lett. **71**, 287 (1993).

[5] J. P. Hill and D. F. McMorrow, Acta Crystallogr. Sec. A **52**, 236 (1996).

[6] E. D. Isaacs, P. Zschack, C. L. Broholm, C. Burns, G. Aeppli, A. P. Ramierez, R. W. Erwin, N. Stücheli, and E. Bucher, Phys. Rev. Lett. **75**, 1178 (1995).

[7] C. Detlefs, A. I. Goldman, C. Stassis, P. C. Canfield, B. K. Cho, J. P. Hill, and D. Gibbs, Phys. Rev. B **53**, 6355 (1996).

[8] G. M. Watson, D. Gibbs, G. H. Lander, B. D. Gaulin, L. E. Berman, H. Matzke, and W. Ellis, Phys. Rev. Lett. **77**, 751 (1996).

[9] R. Nagarajan *et al.*, Phys. Rev. Lett. **72**, 274 (1994); R. J. Cava *et al.*, Nature (London) **367**, 252 (1994); R. Cava *et al.*, *ibid.* **367**, 146 (1994); H. Eisaki *et al.*, Phys. Rev. B **50**, 647 (1994).

[10] T. Siegrist, H. W. Zandbergen, R. J. Cava, J. J. Krajewski, and W. F. Peck, Jr., Nature (London) **367**, 254 (1994).

[11] C. Stassis and A. I. Goldman (unpublished); J. W. Lynn (unpublished), and references therein.

[12] P. C. Canfield, B. K. Cho, D. C. Johnston, D. K. Finnemore, and M. F. Hundley, Physica C **230**, 397 (1994); B. K. Cho, P. C. Canfield, L. Miller, D. C. Johnston, W. P. Beyermann, and A. Yatskar, Phys. Rev. B **52**, 3684 (1995).

[13] J. W. Lynn, S. Skanthakumar, Q. Huang, S. K. Sinha, Z. Hossain, L. C. Gupta, R. Nagarajan, and C. Godart (unpublished).

[14] P. C. Canfield (unpublished).

[15] D. Watson, E. M. Forgan, W. G. Stirling, W. J. Nuttall, S. C. Perry, M. M. R. Costa, and D. Fort, J. Magn. Magn. Mater. **140-144**, 743 (1995).

[16] A. Zheludev, J. P. Hill, and D. J. Buttrey, Phys. Rev. B **54**, 7216 (1996); J. P. Hill, A. Vigliante, D. Gibbs, J. L. Peng, and R. L. Greene, *ibid.* **52**, 6575 (1995).

[17] M. Hamrick, Ph.D. thesis, Rice University, 1994.

[18] H. König (private communication).